Wave energy converter power take-off characterization: comparing dynamometer and field data

Curtis J. Rusch, Corey Crisp, Erik Hammagren, Joe Prudell, and Jim Thomson

Abstract—**We characterize the behavior of a wave energy converter's power take-off unit through dynamometer and field tests. Using the dynamometer with the device in freewheel, we calculate the friction and inertia of the system. We then apply the calculated inertia to data collected with the generator turned on. We develop a linear relationship between shaft speed and observed torque. When this relationship is applied to field data, our predicted torque follows a similar behavior to torque recorded during dynamometer testing. Finally, we emphasize lessons learned form this exercise, noting that the dynamometer control gain impacts the measured torque profile.**

Index Terms—**Wave energy, Dynamometer, Power take-off, point absorber**

I. Introduction

As wave energy converter (WEC) technologies advance, more devices move from the design stage to prototype deployments. As these prototypes increase in size, power take-off units (PTOs) transition from dampers that provide representative loads to actual energy harvesting units. Proper PTO characterization is critical to the understanding of device performance. Laboratory dynamometer testing can allow both characterization and tuning of the PTO and its associated control schemes.

With a wide variety of PTO designs being implemented in WECs, PTO testing has taken on many different forms. This includes hydraulics, direct drive rotary or linear generators, and mechanical power transmission [1]. Bench top PTO testing is cited as a critical step in WEC development, minimizing risk and reducing uncertainty. A study by Simmons, et al. [2] explores the design and validation of a simulated dynamometer that would be required prior to physical implementation. This study is related to the a floating oscillating surge WEC (FOSWEC), and would be mounted to the device during tank testing.

A 5 MW direct drive dynamometer at the National Wind Technology Center was used to characterize LandRAY, a prototype PTO for CPower [3]. Though sparsely reported, this serves as one of few documented examples of dynamometer characterization of a WEC PTO. The report shows a linear relationship between shaft torque and speed when the PTO is actuated using a simulated response in irregular waves. LandRAY is rated for 0.65 MW peak power and 1 MNm peak torque, providing a standalone PTO for CPower to test outside of a WEC [4]. This testing leverages equipment typically used to test PTOs for wind turbines [5], which operate differently than many WECs. Our WEC PTO encounters zero crossing conditions, with acceleration and deceleration of the generator with each passing wave. As such, PTO inertia becomes an important part of the system dynamics, particularly for low-power systems.

This work focuses on the TigerRAY WEC (see Fig. 1), which has a rotary electrical generator. PTO testing is accomplished by coupling of the WEC's drive shaft to our dynamometer in a lab setting. We characterize system friction and inertia and establish a relationship between shaft speed and torque. Through velocity control, we prescribe oscillatory motion using both regular waves and simulated device motion in irregular waves. We develop a relationship between PTO speed and torque for use in a future hydrodynamic model, and we compare the response of the device on the dynamometer to the response during field testing.

II. Methods

A. WEC

TigerRAY, shown in Fig. 1, is a two-body point absorber WEC built by CPower and the University of Washington Applied Physics Lab. The surface body consists of two cylindrical floats connected to a central nacelle. The nacelle contains gearboxes, generators and critical electronics, and is tethered to a heave plate. When activated by waves, the floats rotate about the nacelle, spinning the drive shaft to generate electricity. TigerRAY is about 3 m long, with a nacelle diameter of 1 m and float diameters of about 0.5 m. The heave plate is located approximately 27 m beneath the surface, with a diameter of 2.4 m.

TigerRAY has undergone two years of laboratory and field testing. Thus far, field testing has consisted of 4-6 hour, drifting deployments in Lake Washington and Puget Sound, near Seattle. During wind events, these bodies of water provide small waves that are well scaled to the size of the device. Drifting tests include

This work is supported by the Naval Facilities Engineering Command through NAVSEA Contract No. N00024-21-D-6400.

Curtis Rusch and Jim Thomson are with the Applied Physics Lab at the University of Washington, 1013 NE 40th St, Seattle, WA 98105. (email: curusch@uw.edu)

Corey Crisp is with the Department of Mechanical Engineering, University of Washington.

Erik Hammagren and Joe Prudell are with CPower, in Corvallis Oregon.

Digital Object Identifier:
https://doi.org/10.36688/ewtec-2023-293

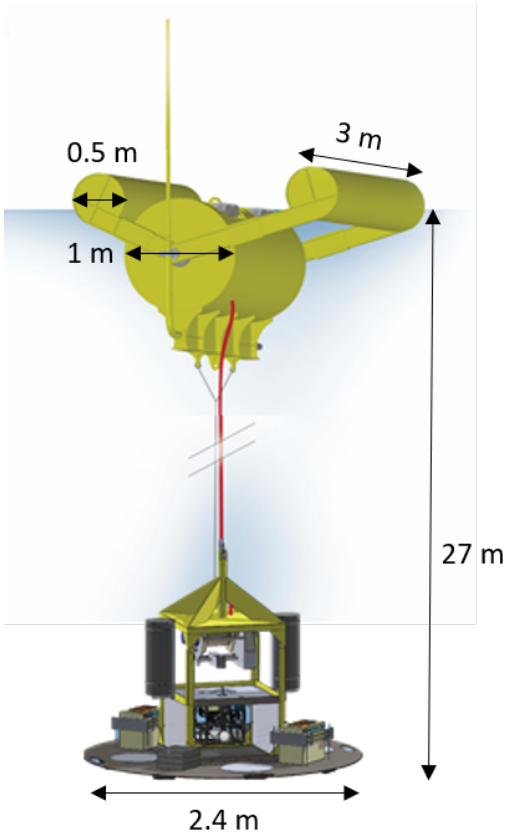

Fig. 1. Schematic of TigerRAY, the WEC used in this study.

periods where the PTOs are engaged and generating power, and periods with the device in freewheel. The aim of these tests is to both assess the performance of the device and gather data for hydrodynamic model validation. Prior to field tests, we characterize the generators and tune our control algorithms using a dynamometer, as presented in the next section.

B. Dynamometer

The dynamometer used to characterize the TigerRAY power take-off (PTO) is shown in Fig. 2. The driving motor is a Siemens 1FW3202-1.E torque motor with a rated speed of 150 rpm and a rated torque of 500 Nm. Our WEC generator is designed for high torque-low speed actuation, so we couple the two using a 5:1 gearbox, increasing torque and decreasing speed between the motor and generator. Between the gearbox and WEC driveshaft, we use a Himmelstein bearingless digital torque meter with a 2200 Nm torque range. To couple the drive shafts, we use high-stiffness, backlash-free R+W disc pack couplers. For this work, we operate the dynamometer using velocity control.

Prior to field deployment, the dynamometer is used to characterize and tune the response of our WEC's PTO. For this process, we first run constant-speed tests, where we step through the full range of anticipated operating speeds, holding constant velocity for at least 5 seconds at each velocity step. A portion of the time series from one of these tests is shown in Fig. 3. We the run a range of sinusoidally varying velocity tests. These tests allow us to repeatably target speeds of

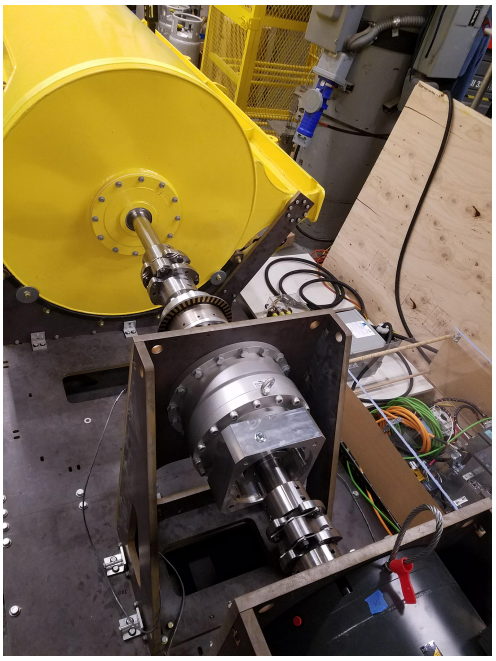

Fig. 2. The APL dynamometer coupled to the port side drive shaft of the TigerRAY nacelle during testing in 2022.

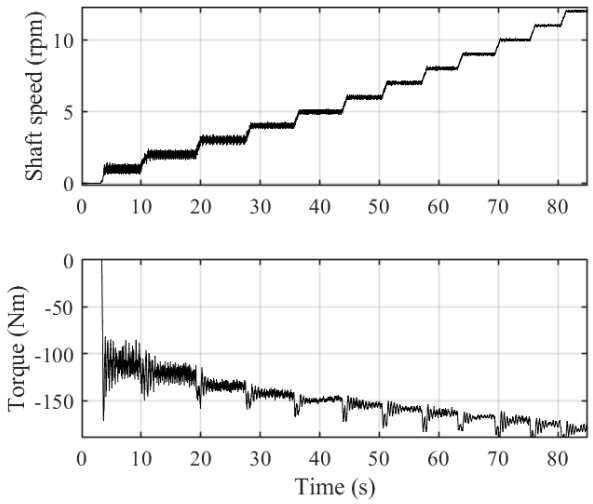

Fig. 3. Example of speed and torque measured during constant-speed tests.

interest. Finally, we run irregular velocity tests. For these tests, we use a time series of velocity simulated by CPower. We conduct constant speed tests with the PTO in freewheel and engaged.

C. Data analysis

In this section, we step through the data processing used to analyze data from both dynamometer and field tests. Torque applied to the drive shaft is measured by our torque cell, and we refer to this as τ_{meas}. Additionally, use the dynamometer encoder to measure shaft angle, which is differentiated to calculate shaft angular velocity (ω) and angular acceleration (α).

Through dynamometer testing, we first calculate PTO friction torque (τ_f) in freewheel. To accomplish this, we bin the data from our constant-speed tests into 25 bins (corresponding to the number of velocity

steps from testing). In MATLAB, we discretize the data into the closest bin, and then calculate the 25^{th}, 50^{th}, and 75^{th} percentile values in each bin. This data is symmetric, and to calculate friction for future steps, we use the 'interp1' function with shape-preserving piecewise cubic interpolation (pchip) to interpolate binned data, using binned friction as a function of positive shaft speed as reference data.

Next, we calculate inertia with the PTO in freewheel. To do this, we run a time series of both sinusoidal and irregular shaft speeds. From these tests, we calculate inertia assuming that τ_{meas} consists of two terms: friction (τ_f) and inertia (τ_i). Since we are measuring torque, and we have a measurement of the friction, we can solve for inertia as:

$$\tau_i = \tau_{meas} - \tau_f \tag{1}$$

We can write the torque due to inertia as $\tau_i = I\alpha$, where I is the moment of inertia of the WEC PTO unit, and α is the rotational acceleration of the WEC drive shaft. Rearranging equation 1, we can now solve for the PTO's moment of inertia as

$$I = \frac{\tau_{meas}(t) - \tau_f(t)}{\alpha(t)} \tag{2}$$

where each term on the right side of the equation is a function of time, t. We use the backslash operator in MATLAB to take the least squares fit to equation 2 for each test.

Next, with the PTO engaged, we once again bin data from constant-speed tests to build a torque-speed relationship of the PTO. From this data, we produce a linear fit to the low-speed data (between -2 and +2 rpm) using a least squares fit. Since shaft speed remains within this operation region for a majority of the field data, we neglect the secondary linear response for higher shaft speeds for this fit. To test the accuracy of this fit, we reconstruct the torque expected with this approximation as

$$\tau_{fit}(t) = I\alpha(t) + \tau_{PTO}(\omega(t)), \tag{3}$$

where $\tau_{PTO}(\omega(t))$ is the non-inertial PTO torque calculated from our linear fit to the low-speed dat, which is a function of shaft speed, ω.

III. Results

A. Friction and inertia characterization

First, we characterize the friction and inertia of the system in freewheel. In simulation, such a characterization allows validation of model hydrodynamics without the added complexity of PTO forcing. To conduct freewheel tests, we command the dynamometer to step through the expected range of operating speeds, holding the WEC PTO speed constant for about 5 seconds for each speed step. For this test, we step through speeds from -12 to 12 rpm on the WEC drive shaft in increments of 1 rpm. As shown in Fig. 4, these tests exhibit high repeatability. We interpolate the binned data to calculate friction as a function of shaft speed in the freewheel case. This fit is shown as the dark blue line in Fig. 4.

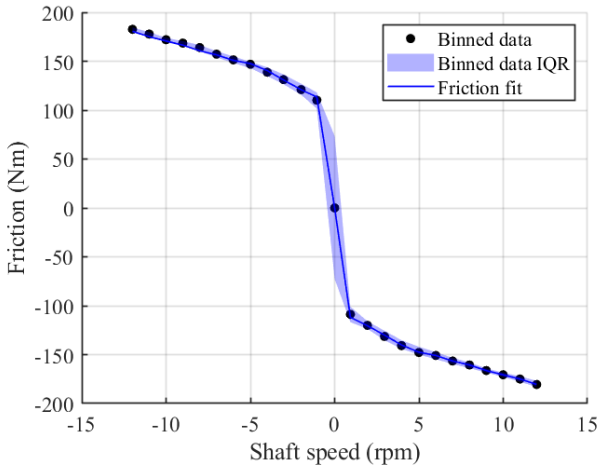

Fig. 4. Friction data from freewheel dynamometer tests, overlaid with the interquartile range and the line of best fit to the data.

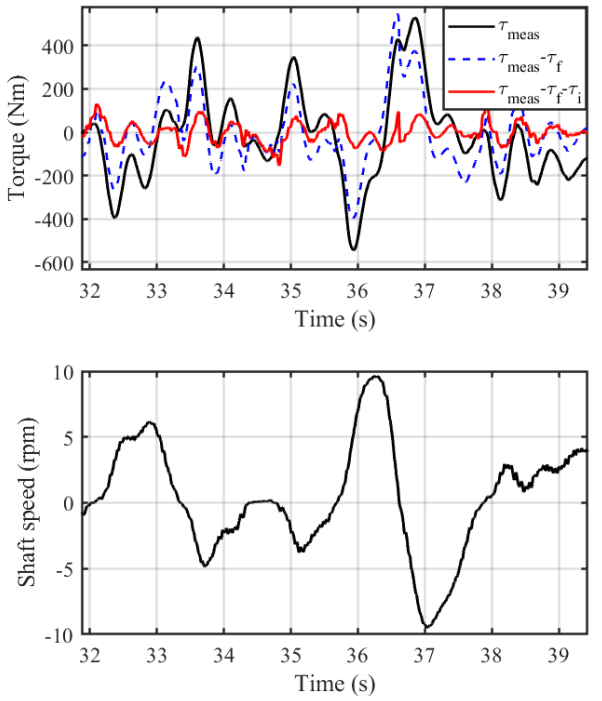

Fig. 5. Comparison of measured torque, residual torque when subtracting our friction approximation, and residual torque when subtracting both approximated friction and inertia. This dynamometer test was controlled using expected operational speeds in an irregular wave field with $H_s = 0.5$ m and $T_p = 3.2$ s. These expected speeds were determined with proprietary hydrodynamic modeling conducted by CPower.

Building on the friction characterization, we calculate PTO inertia using freewheel tests driven with sinusoidal and irregular oscillatory velocities. Across both sinusoidal and irregular oscillations, we calculate a moment of inertia of 106 kg m^2, ± 5 kg m^2. As shown in Fig. 5, these approximations account for nearly all of the measured force in these tests. The residual force has an inter-quartile range that spans -40 to 40 Nm for our irregular wave test. This means that, on average, this representation captures about 90% of the measured

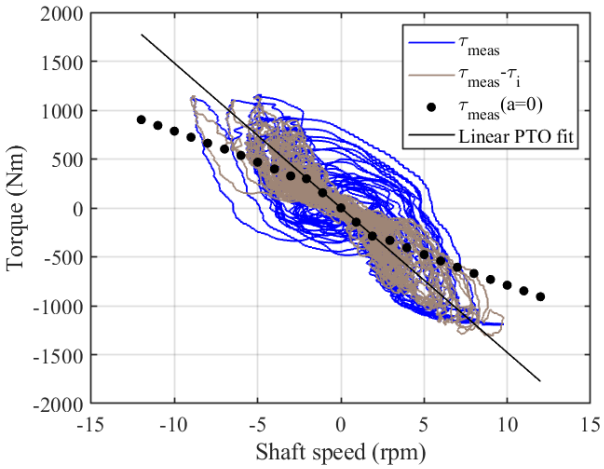

Fig. 6. Measured torque from constant velocity tests, compared with torque measured during an irregular wave case with and without accounting for freewheel inertia. The black line represents a linear fit to the low-speed constant velocity torque data.

force.

B. PTO characterization

In addition to freewheel tests of the system, we characterize performance with the PTO on. As with freewheel, we begin our analysis by collecting constant speed torque data while cycling through the full range of operating speeds. Comparing this with torque measured during our operational irregular wave case, a clear trend emerges. As shown in Fig. 6, the data collected at constant velocity exhibits piece-wise behavior. This is due to the PTO architecture, which contains two power electronics units - a low-power and high-power unit. We see a discontinuity in the constant velocity data where the transition between PTO units takes place. Using the moment of inertia from freewheel testing and the measured acceleration, we calculate the inertia of the motor. This is subtracted from the measured torque, yielding a torque-speed plot that displays a fairly linear trend (shown by the grey line in Fig. 6). To model the response linearly, we use the torque-speed relationship in the low-speed region of our plot. The extension of this linear representation is shown by the black line in Fig. 6.

Using this linear representation and our characterized generator inertia, we reconstruct the measured torque as a function of drive shaft speed. Shown in Fig. 7, this reconstruction tracks the measured torque closely. On average, this reconstruction over-predicts the magnitude of peak forces by 10%, and under-predicts torques between -500 Nm and 500 Nm by 10-20%. This provides a relatively high-fidelity relationship that can be used in a hydrodynamic model to specify the torque provided by the PTO as a function of shaft speed.

C. Comparison to field data

To assess the validity of our dynamometer data, we use data taken from field testing of our WEC. In the field, we have no way to measured the torque on the system, so we rely on our torque-speed relationship to understand the torques applied to the WEC by waves. We make this comparison with data from field testing in natural waves on Lake Washington from February 7, 2023. During this field test, significant wave height approaches 0.4 m, with a peak period of 2.4 s. The shaft speeds from the field are smaller than the original magnitudes explored in section III-B. As such, our closest comparison to field data comes from dynamometer tests using a commanded velocity with one quarter the amplitude of the original time series. Using equation 3, our calculated PTO inertia (I), the linear PTO torque fit (τ_{PTO}) and the shaft speed ($omega$) and acceleration ($alpha$) calculated from measured shaft position, we calculate τ_{fit} for our WEC deployed in irregular waves. In Fig. 6, we see that the torque-speed data collected on the dynamometer using quarter scale seas match our predicted torque-speed relationship from field data closely.

To further verify our comparisons, we look at the statistical distribution of shaft speed in the field and on the dynamometer. Shown in Fig. 9, the probability distribution for the dynamometer data and field data match closely. This data indicates that we are modelling shaft speed accurately, and that our model for torque provides a predicted torque from field data that matches our measured torque on the dynamometer. The main difference between the two probability distributions is in the near-zero velocity region. This discrepancy is likely due to two differences between dynamometer and field tests. First, the dynamometer is velocity controlled, so it provides enough torque to motor past low-speed regions where friction causes stiction in the field. Second, the effect of stiction was not modelled, since the model was created prior to construction of the device, and the magnitude of friction was not known. As a result, there are more periods of zero velocity in the field than on the dynamometer, and a corresponding difference in near-zero velocities.

IV. Discussion

Some nuance in the dynamometer settings can impact these results. For example, during our first round of dynamometer testing, we discovered that the dynamometer controller's proportional gain was too high. As a result, it acted too 'strongly', overemphasizing the importance of following the commanded velocity. For tests where drive shaft speeds exceed about 4 rpm, this results in an unusual response in the measured torque. As shown in Fig. 10, we see that torque hits a 'ceiling' shy of the maximum value recorded in the low gain case. For a low gain, we see more noise in our velocity signal, but a smooth torque peak. In dynamometer testing, a trade-off occurs between torque and velocity. Since we are operating in a velocity-control mode, when we follow commanded velocity closely, we have limitations with our measured torque. Conversely, reducing the control gain results in a noisier velocity, but a smoother torque measurement. As such, we recommend giving thought to the reactivity of the dynamometer control, since it has implications for the characterization of the system. Another

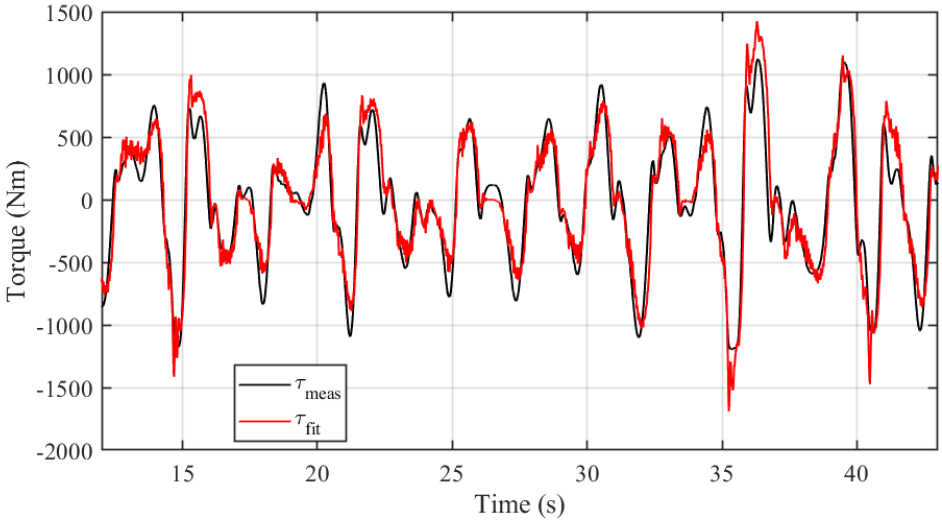

Fig. 7. Torque measured during an irregular wave test, compared to torque reconstructed using a linear fit and our freewheel-derived moment of inertia.

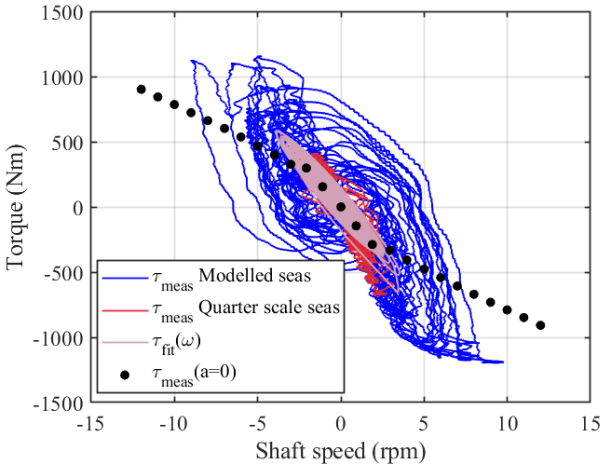

Fig. 8. Torque measured during an irregular wave dynamometer test for two different oscillation amplitudes, compared with torque calculated shaft velocity measured in the field. For context, constant-velocity measurements of PTO torque are overlaid.

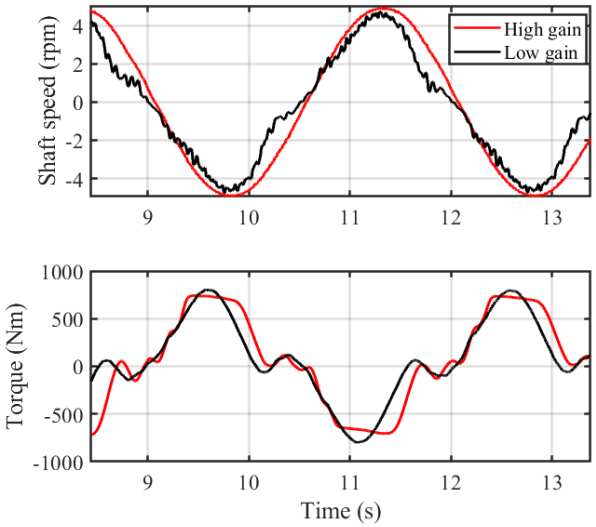

Fig. 10. Comparison of recorded shaft speed and torque when the dynamometer is set with high and low gains.

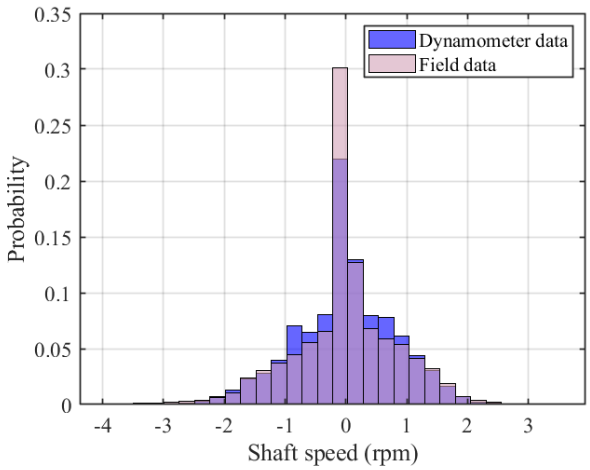

Fig. 9. Probability of occurrence for shaft speeds in our field data and data taken on the dynamometer using the quarter scale command velocity.

approach is torque-control, however this requires prior knowledge of the torque-speed relationship, and in general, torque control comes with a risk of runaway speeds on the dynamometer if the PTO enters a load-shedding operation regime.

V. Conclusion

In this work, we outline the dynamometer testing that was conducted to characterize the freewheel friction and inertia of the TigerRAY WEC PTO. We then use this inertia characterization to analyze dynamometer data taken with the PTO engaged. Accounting for this inertia reduces the scatter of the torque-speed relationship, and bolsters the use of a linear torque-speed fit. We show that this fit generally over-predicts peak forces by 10% and under-predicts lower torques by about 10-20%. Using this fit, we calculate the predicted torque on the drive shaft from shaft speeds recorded

during field tests. This shows that the expected torque-speed relationship, when accounting for PTO inertia, is similar to dynamometer tests run using quarter scaled input speeds. Since the wave conditions during field tests were smaller than the original modelled seas, this provides validation that dynamometer testing with reduced speeds accurately represents conditions experienced by the WEC. Finally, we comment on the nuance of dynamometer tests. We specifically show the impact of the dynamometer's PID gains, where an over-reactive dynamometer causes irregularities in the applied torque. Future work will apply the relationships we have developed to hydrodynamic models of the WEC, allowing for validation of these models using field data.

ACKNOWLEDGEMENT

We acknowledge the work done by Zhe Zhang of CPower, who modelled TigerRAY and provided us with a time series of modelled shaft speed that was used in dynamometer testing. Additional work by Kelen O'Hearn, and many other CPower employees, was critical to the design and manufacture of TigerRAY. APL employees Jesse Dosher, Harlin Wood, and Chris Bassett were critical to the setup and troubleshooting of the dynamometer, and the original design of the dynamometer was made possible by the work of Paul Gibbs. Finally, field testing of the TigerRAY wouldn't have been possible without numerous APL employees, including Alex DeKlerk, Joe Talbert, and Emily Iseley.

REFERENCES

[1] N. Tom, "Review of wave energy converter power take-off systems, testing practices, and evaluation metrics: Preprint," National Renewable Energy Laboratory, Golden, CO, Tech. Rep. NREL/CP-5700-82807, 2022. [Online]. Available: https://www.nrel.gov/docs/fy23osti/82807.pdf

[2] A. Simmons, T. K. A. Brekken, P. Lomonaco, and C. Michelen, "Creating a dynamometer for experimental validation of power take-off forces on a wave energy converter," in *2015 IEEE Conference on Technologies for Sustainability (SusTech)*, 2015, pp. 148–153.

[3] J. Keller, "Test of a novel, commercial-scale wave energy direct-drive rotary power take-off at the NREL National Wind Technology Center: cooperative research and development final report," National Renewable Energy Laboratory, Golden, CO, Tech. Rep. NREL/TP-5000-76906, 2020. [Online]. Available: https://www.nrel.gov/docs/fy20osti/76906.pdf

[4] K. Rhinefrank, A. Schacher, J. Prudell, E. Hammagren, A. von Jouanne, and T. Brekken, "Scaled development of a novel wave energy converter through wave tank to utility-scale laboratory testing," in *2015 IEEE Power Energy Society General Meeting*, 2015, pp. 1–5.

[5] "Wind research - dynamometer research facilities," accessed on June 05, 2023. [Online]. Available: https://www.nrel.gov/wind/facilities-dynamometer.html